Separation Science and Technology

ISSN: 0149-6395 (Print) 1520-5754 (Online) Journal homepage: http://www.tandfonline.com/loi/lsst20

Adsorption/Desorption of Hg(II) on FDU-1 Silica and FDU-1 Silica Modified with Humic Acid

Luis Carlos Cides da Silva, Carlos M. C. Infante, Ricardo de Prá Urio, Ivana Conte Cosentino, Marcia Carvalho de Abreu Fantini, Jivaldo do Rosário Matos, Fernando H. do Nascimento & Jorge C. Masini

To cite this article: Luis Carlos Cides da Silva, Carlos M. C. Infante, Ricardo de Prá Urio, Ivana Conte Cosentino, Marcia Carvalho de Abreu Fantini, Jivaldo do Rosário Matos, Fernando H. do Nascimento & Jorge C. Masini (2015) Adsorption/Desorption of Hg(II) on FDU-1 Silica and FDU-1 Silica Modified with Humic Acid, Separation Science and Technology, 50:7, 984-992, DOI: 10.1080/01496395.2014.983246

To link to this article: http://dx.doi.org/10.1080/01496395.2014.983246

Accepted author version posted online: 11 Feb 2015.
Published online: 11 Feb 2015.

Separation Science and Technology, 50: 984–992, 2015

ISSN: 0149-6395 print / 1520-5754 online
DOI: 10.1080/01496395.2014.983246

Taylor & Francis
Taylor & Francis Group

Adsorption/Desorption of Hg(II) on FDU-1 Silica and FDU-1 Silica Modified with Humic Acid

Luis Carlos Cides da Silva,[1] Carlos M. C. Infante,[2] Ricardo de Prá Urio,[1] Ivana Conte Cosentino,[3] Marcia Carvalho de Abreu Fantini,[4] Jivaldo do Rosário Matos,[1] Fernando H. do Nascimento,[1] and Jorge C. Masini[1]

[1]*Instituto de Química, Universidade de São Paulo, São Paulo, SP, Brazil*
[2]*Faculdade de Ciências Farmacêuticas, Curso de Ciência Farmacêuticas, Brasília, DF, Brazil*
[3]*Instituto de Pesquisas Energéticas e Nucleares, São Paulo, SP, Brazil*
[4]*Instituto de Física, Universidade de São Paulo, São Paulo, SP, Brazil*

Incorporation of humic acid in the FDU-1 mesoporous silica improved Hg(II) adsorption and did not destroy the ordered network, providing surface area of 500 m^2 g^{-1}, pore volume of 0.9 cm^3 g^{-1}, and mean pore diameter of 10 nm. Carboxylic and phenolic groups increased the affinity by forming surface complexes with Hg(II). Isotherms (25.0 ± 0.1°C) were fitted to the Freundlich equation, exhibiting K_f values that increased with pH and 1/n that decreased to values < 1 with the heterogeneity of sites. Hg(II) desorption in 0.10 mol L^{-1} acetic acid was lower than 10%, suggesting that chemisorption processes govern the Hg(II) removal.

Keywords FDU-1 silica; Hg(II) adsorption; humic acid; voltammetry; ordered mesoporous silica

INTRODUCTION

Mercury is one of the most toxic metals, demanding much attention because of its impact on public and environmental health. Main anthropogenic sources include wastewater discharges and atmospheric deposition from mining activities, oil and coal combustion, chloro-alkali industries, cement production, municipal waste, sewage sludge combustion, and manufacture of batteries (1–2). Technologies for the removal of aqueous mercury include precipitation, coagulation, reduction, membrane separation, ion exchange, and adsorption (3, 4). Adsorption is an interesting approach because of its effectiveness and low cost. Among the adsorbents studied, special attention has been given to activated carbons (5), silicates (6–8), polymers (9, 10), biomass (11), and chitosan (12, 13). Natural minerals have also being extensively studied (14, 15).

Received 28 Feburary 2014; accepted 29 October 2014.
Address correspondence to Jorge C. Masini, Instituto de Química da Universidade de São Paulo, P.O. Box 26077, 05513-970, São Paulo, SP, Brazil. E-mail: jcmasini@iq.usp.br

Organofunctional molecules anchored on various surface supports such as natural silica and silicate, synthetic materials and mesoporous silica have been used for trace metal separation and concentration methodologies (8, 16–18). As the organic groups bound to silica matrix have basic donor reactive atoms, an improvement in adsorption and exchange properties may be achieved in comparison with the unmodified support material (6–8, 16–18). Materials effective for mercury removal generally carry sulfur (3, 4, 8, 16, 17), nitrogen, and oxygen (8, 10) containing functional groups as major binding sites for mercury.

Because of its abundant occurrence in soils, sediments, and water, natural organic matter (NOM) is a potentially interesting modifier of silica surfaces, simulating a natural environmental process. Natural organic matter (NOM) is predominantly constituted by humic and fulvic acids, which are rich in carboxylic and phenolic ionizable groups. Cides da Silva et al. (19, 20) modified FDU-1 silica with humic acid, verifying a significant increase in the adsorption capacity of this mesoporous silica toward adsorption of Cd^{2+} (19, 20), Pb^{2+}, and Cu^{2+} (20). Lee et al. (21) studied the relative roles of the mineral surface and dissolved organic matter in controlling Hg(II) adsorption at the muscovite (001)-solution interface using interface-specific X-ray reflectivity combined with element specific resonant anomalous X-ray reflectivity in the presence and absence of fulvic acids. Both inner- and outer-sphere complexes were formed with the mineral surface at pH 2.0. Adsorption of Hg(II) is enhanced if the mineral is previously modified by fulvic acid; on the other hand, adsorption on the mineral surface decreases if the complex of fulvic acid with Hg(II) is formed in solution, prior to addition of the mineral. Adsorption of the Hg(II)-fulvic acid complexes at the mineral surface decreased as the pH increased.

Highly ordered cubic cage-like mesoporous silica, named FDU-1, is synthesized from tetraethyl orthosilicate (TEOS) in the presence of poly(ethylene oxide)–poly(butylene

oxide)–poly(ethylene oxide) triblock copolymer (PEO–PBO–PEO) in a strong acidic medium (22, 23). FDU-1 has a BET surface area of about 740 m^2 g^{-1}, a large pore size (ca. 12 nm), pore volume of 0.8 cm^3 g^{-1} and wall thickness between 2.9 and 7.4 nm. Its exceptionally high thermal and hydrothermal stability can be attributed to the combination of its large wall thickness and the continuous 3-dimensional nature of its thick wall backbone (24). Matos et al. (25) showed that FDU-1 has a porous cubic *Fm3m* structure with a 3-D hexagonal intergrowth, similar to SBA-2 and SBA-12 (25). It was demonstrated that the temperature and time control during the synthesis allow to gradually change the cage-like pores of FDU-1 to a highly open and accessible porous system with a narrow pore width distribution (22–25). The synthesis process requires hydrothermal treatment, which can be efficiently performed in a microwave oven (26). In this work, the FDU-1 silica was prepared with a new triblock copolymer Vorasurf 504® $(EO)_{38}(BO)_{46}(EO)_{38}$ (26).

This paper describes adsorption studies of Hg(II) on FDU-1 silica and FDU-1 silica modified with humic acid as a function of pH under conditions of low site occupation. Desorption studies in the adsorption medium and in 0.10 mol L^{-1} acetic acid were made to evaluate the stability of the surface complexes formed with either the silanol or carboxylic/phenolic groups of FDU-1 supported humic acid (28). The idea of using a cage-like type of ordered mesoporous silica reservoir relies on the ability of this type of structure to hold and to isolate harmful compounds.

EXPERIMENTAL

Humic Acid Preparation

15 g of sodium salt of HA from Aldrich were dissolved in 100 mL of 0.1 mol L^{-1} NaOH solution under N_2 atmosphere. After 15 min the suspension was centrifuged at 1000 rpm for 30 min and the supernatant phase was acidified to pH 1.0 with 6 mol L^{-1} HCl. The suspension was centrifuged and the precipitated HA was washed with deionized water four times for the removal of salt excess. Finally, the solid phase that consisted of HA was re-suspended in 250 mL of deionized water. The HA concentration in this stock suspension was 28.0 ± 0.6 g L^{-1}, which was determined gravimetrically by drying 1.00 mL aliquots. The ash content was (8.0 ± 0.5)% and the elemental composition of the dry HA was: (49.7 ± 0.1)% C, (4.3 ± 0.1)% H, and (0.65 ± 0.02)% N determined by using the elemental analyzer 2400 instrument from Perkin Elmer. To facilitate the handling of the HA suspension, and its subsequent incorporation in FDU-1, the pH of a 25.00 mL aliquot was adjusted to 7.5 using 1.0 M $NaHCO_3$ solution followed by its dilution to 50.00 mL, which gave the final HA concentration of 14.0 g L^{-1} (19, 20).

FDU-1 and FDU-1/ HA Synthesis

The synthesis of the FDU-1 samples was carried out using the same synthesis gel composition as reported by Cides da Silva et al. (27): 1 TEOS: 0.00755 Vorasurf 504®: 6 HCl: 155 H_2O, where TEOS stands for tetraethylorthosilicate from Aldrich Chemical Company, Vorasurf 504® is a poly(ethylene oxide)-poly(butylene oxide)-poly(ethylene oxide) triblock copolymer $(EO)_{38}(BO)_{46}(EO)_{38}$ from Dow Chemicals. In a synthesis procedure, 2 g of Vorasurf 504® copolymer was dissolved in 120 g of 2 mol L^{-1} HCl and stirred at room temperature until a homogeneous mixture was obtained. Subsequently, 8.32 g of TEOS, 30 mL of 14 g L^{-1} humic acid (HA) solution, respectively, were added. The resulting mixture was vigorously stirred in an open beaker for 24 hours at room temperature. The precipitation was observed in 30–40 min after the addition of TEOS and HA solution. The obtained mixture was transferred into a Teflon vessel and heated under autogenous pressure for 24 h at 100°C. Finally, the precipitate was filtered out, washed with ethanol, and dried at 25°C. The template inside the as-synthesized samples was removed by soxhlet extraction at boiling point for 12 h using ethanol to yield FDU-1/HA and FDU-1. The pure silica samples are denoted as FDU-1, whereas the HA incorporated materials are denoted as FDU-1/HA EX. The samples were named "AS," denoting the as-synthesized state with copolymer (and HA) inside the pores and named "EX," after template extraction.

Thermogravimetry

TG/DTG curves were obtained with a thermobalance model TGA 50 (Shimadzu) in the temperature range 25–900°C, using platinum crucibles with ∼3 mg of samples, under dynamic nitrogen atmosphere (50 mL min^{-1}) and heating rate of 10°C min^{-1}.

Small Angle X-Ray Scattering (SAXS)

The Small Angle X-Ray Scattering (SAXS) experiments were carried out in a Nanostar from Bruker, using a two-dimensional filament detector. The samples were analyzed inside a mechanical vacuum chamber (∼10^{-2} Torr) in order to avoid scattering from air. The data were normalized by removing the parasitic scattering from the sample holder and corrected due to absorption. The measurements were performed with monochromatized, by Göbel X-ray mirrors, Cu Kα radiation (λ = 0.15418 nm), 1.5 kW, in the q range of 0.13 to 3.4 nm^{-1} and 40 min exposure time.

Nitrogen Adsorption Isotherms

Adsorption isotherms were measured with Micromeritics ASAP 2010 volumetric adsorption analyzer using nitrogen of 99.998% purity. Measurements were performed in the range of relative pressure from 10^{-6} to 0.99 liquid nitrogen on the samples degassed for 2 hours, under vacuum of about 10^{-3} Torr, at 110°C. The degassing temperature (110°C) was selected to avoid the decomposition of attached organic ligands and ensure thermodecomposition of physically adsorbed water. The

specific surface area was evaluated using BET method (29). The total pore volume was estimated from the amount adsorbed at the relative pressure of 0.99. The pore size distribution (PSD) was calculated using BJH algorithm (30), with the relation between the capillary condensation pressure and the pore diameter established by Kruk et al. (31).

Hg(II) Adsorption/Desorption Studies

Adsorption studies were made in FDU-1 EX or FDU-1/HA EX suspensions containing 0.0250 ± 0.005 g of sorbent in 5.0 mL of Hg(II) solutions of initial concentrations of 20, 30, 40, 50, 100, and 200 μmol L^{-1}, prepared in pH 2.0, 4.0, or 6.0. A 0.010 mol L^{-1} HNO_3 solution was used for experiments at pH 2.0; pH 4.0 was obtained by preparing the solutions in 0.10 mol L^{-1} acetic acid/sodium acetate buffer (ratio $[HAc]/[Ac^-] = 5.6$); pH 6.0 was obtained by preparing the solutions in 0.10 mol L^{-1} 2-[N-morpholine]-ethanesulfonic acid (MES, pK_a 6.15). These suspensions were prepared in 15 mL Corning® (Lowell, MA, USA) centrifuge tubes. A blank experiment, without the presence of an adsorbent, was carried out in parallel for each sample. All tubes were closed and maintained under gentle shaking for 24 h at 25.0 ± 0.1°C in a thermostatic orbital shaker. After that, the tubes were centrifuged at 2600 *g* for 15 min, and 4.50 mL of the supernatant solutions were transferred to vials and stored in a refrigerator (4°C) for further determination of the free concentrations of Hg(II).

The adsorbent remaining in the tubes was subjected to desorption experiments. A first desorption step was performed in a medium similar to that used for adsorption, that is, for the pH 2.0 experiment, 4.50 mL of the 0.010 mol L^{-1} HNO_3 were transferred to the tubes (completing the total volume to 5.0 mL). Suspensions were stirred again for 24 h at 25.0 ± 0.1°C. As previously described, the suspensions were centrifuged at 2600 *g* and the supernatants were stored for determination of free Hg(II). Similar desorption procedures were made with 0.10 mol l^{-1} acetic acid/sodium acetate buffer and 0.10 mol L^{-1} MES to evaluate desorption at pH 4.0 and 6.0, respectively. A further desorption step was made in 0.10 mol L^{-1} acetic acid for two hours in all tubes, independently of the initial adsorption pH.

Voltammetric Determinations of Hg(II)

All reagents were of analytical grade and the working solutions were prepared in deionized water obtained from the Simplicity 185 system from Millipore (Billerica, MA, USA) coupled to an UV lamp. Stock 1000 mg L^{-1} standard solution of Hg(II) was bought from Merck. Working solutions were prepared by dilution of this stock with deionized water.

Voltammetric measurements were carried out using a model 263A potentiostat/galvanostat from Princeton Applied Research (Oak Ridge, Tennessee, USA). A MF2014 1.6 mm diameter disk gold electrode from Bioanalytical Systems, Inc. (West Lafayete, IN, USA) was used as working electrode. The electrochemical cell was completed with an Ag/AgCl reference electrode (KCl saturated) and a platinum auxiliary electrode. Prior to use, the working electrode was manually polished to mirror-like surface with 1.0 μm diamond suspension on metallographic cloth (Arotec S/A, São Paulo, Brazil) and sonicated for 5 min in deionized water. This procedure was repeated using a 0.25 μm diamond suspension, followed by a final 5 min sonication in ethanol. Electrochemical activation of the gold electrode was made in 0.10 mol L^{-1} $HClO_4$ by applying a conditioning potential of 0.90 V vs Ag/AgCl for 60 s followed by two successive cyclic voltammetry experiments:

i. twenty 0.0 V→ 1.5 V → 0.0 V scans at 1.0 V s^{-1} and
ii. ten 0.0 V → 1.0 → 0.0 V scans at 0.10 V s^{-1} with a potential increment of 2 mV in both cases (17, 32, 33).

Voltammetric parameters for determinations of free Hg(II) were adapted from previously described methodologies (17, 32–34). All analyses were made in 0.060 mol L^{-1} HCl (33, 34). Electrochemical conditioning of the working electrode was made by applying 0.90 V for 20 s, followed by a deposition time of 120 s at 0.30 V. Anodic stripping was made scanning the potential from 0.30 to 0.90 V by Square Wave Voltammetry (SWV) using 25 mV of pulse height, frequency of 100 Hz, and scan increment of 2 mV. Voltammograms of sample solutions were subtracted from that of the blank (0.060 mol L^{-1} HCl) and smoothed by a factor 10 sliding average approach provided by the Model 270/250 Research Electrochemistry Software from Princeton Applied Research. Quantification of the free Hg(II) concentrations was made by external calibration using calibration curves constructed daily in the concentration range between 2 and 120 μg L^{-1} (10–600 nmol L^{-1}) in 0.060 mol L^{-1} HCl. Analyses of the samples were made by adding 1.0 mL of 0.30 mol L^{-1} HCl, a sample volume that varied from 0.050 to 1.0 mL of sample (solution coming from adsorption or desorption study) and a proper volume of deionized water to reach a total of 5.0 mL inside the electrochemical cell.

Adsorption Data Treatment

Adsorption data was treated by the linearized Freundlich equation:

$$\log(q) = \log K_f + (1/n)\log[Hg^{2+}]$$

where q is the load of Hg(II) adsorbed in the solid phase (μmol g^{-1}), $[Hg^{2+}]$ is solution concentration (μmol L^{-1}) after the contact time of 24 h, and K_f and 1/n are empirical constants related to adsorption.

RESULTS AND DISCUSSION

Characterization of FDU-1 Materials

Thermogravimetric (TG) curves of the four materials are shown in Fig. 1. Mass variation (Δm), temperature ranges (T_R) and the peak temperatures (T_p) regarding the TG and differential themogravimetric (DTG) experiments are listed in Table 1.

The TG curves (Fig 1a) indicate that the thermal decomposition process of the as-synthesized sample (FDU-1 AS) occurred in three mass loss steps (Table 1). The first step is due to the elimination of physically adsorbed water, the second step corresponds to template elimination, and the third mass loss is related to dehydroxylation process.

For the sample submitted to an extraction process of the template with a solvent (FDU-1 EX), the TG curve (Fig. 1b) indicates that the thermal decomposition of the polymeric template occurs in only one mass loss step with a small mass variation, showing that part of the template is retained inside the material after the extraction process in ethanol. The release of physically adsorbed water and the step of dehydroxylation are similar to those observed for the FDU-1 AS sample.

In the case of FDU-1/AH AS sample, the TG curve (Fig. 1c) shows three stages of mass loss (Table 1), including a mass variation, named Δm_2, which corresponds to the simultaneous thermal decomposition of the template, and humic acid. Values of Δm_1 and Δm_3 correspond, respectively, to the elimination of physically adsorbed water and to the step of dehydroxylation.

The TG curve of the FDU-1/HA EX sample (Fig 1d) shows two stages of thermal decomposition of the template with humic acid (Δm_2). In this case the mass losses are smaller, because the decomposition products were eliminated in the extraction process with ethanol. The steps corresponding to physically adsorbed water elimination and dehydroxylation were similar to those observed for FDU-1/HA AS sample. The comparison between the DTG curves of the four samples shows that the decomposition process of the template and humic acid occurs at temperatures higher than that of the pristine FDU-1 (see Table 1). The removal of the template (including HA) by making use of ethanol showed an efficiency of 91% for the FDU-1 EX sample and 79% for FDU-1/HA EX.

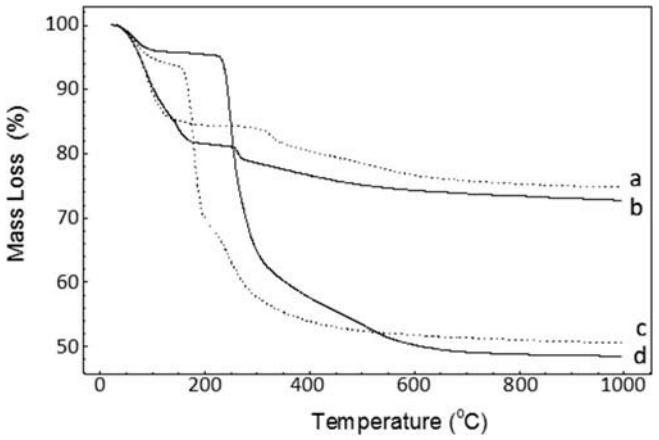

FIG. 1. TG curves for (a) as-synthesized FDU-1 EX, (b) FDU-1/HA EX, (c) FDU-1 AS, and (d) FDU-1/HA EX samples.

The SAXS results depicted in Fig. 2 show that the use of HA in the synthesis induced a more disordered porous structure, since less defined diffraction peaks were detected. The increase in this disorder is also seen by the increase of scattering at low q values. The solvent extraction process shrank the structure since the (111) diffraction peaks were at higher q. The lattice parameter determined with the (111) reflection, shown on Table 2, revealed that the HA inflated the porous network, as expected by the fact that it is included in the synthesis together with the silicon source and it is incorporated on the final structure.

The nitrogen adsorption isotherms of FDU-1 EX and FDU-1/HA EX are shown in Fig. 3a. Both samples exhibit a cage-like type of porous structure with deformations at the pore entrance (25). However, the adsorption capacity and the capillary condensation stage were similar to those commonly observed for FDU-1 (25–27). Despite the lower steepness of the capillary condensation at the relative pressure of 0.7 compared to other reported results (25–27), the prepared samples still have a good uniformity of pore sizes. The FDU-1 EX showed a BET surface area of 570 $m^2\ g^{-1}$ and a total pore volume of 0.67 $cm^3 g^{-1}$; the FDU-1/ HA EX sample presented a BET surface area of 513 $m^2 g^{-1}$ and a total pore volume of 0.87 $cm^3 g^{-1}$. A comparison of the textural results shows that the humic acid improves the properties of the material, since its adsorption capacity remained at high figure, while the pore volume and mean pore diameter increased, as shown in Table 2. The large hysteresis loop illustrates a deformed shape for the FDU-1 EX sample and it is partially deformed for the FDU-1/HA EX sample. The observed hysteresis loop is typical of materials with cage-like cubic structure (25–27). The nitrogen adsorption isotherms of FDU-1 EX and FDU-1/HA EX samples are shown in Fig. 3a. Selected structural and textural parameters are listed in Table 2. The pore size distribution (PSD) of the samples was calculated from nitrogen adsorption isotherms using a calibration method for cylindrical mesopores (31). The PSD are shown as insert in Fig. 3b, and the maximum positions of the peaks of these distributions are listed in Table 2.

Adsorption and Desorption of Hg(II)

Because the equilibrium of adsorption may take from minutes to some hours to be established (19, 20), a 24 h contact time was adopted in the present work. Figure 4 shows the adsorption percentages of Hg(II) on both FDU-1 EX and FDU-1/HA EX materials as a function of the initial Hg(II) concentration and solution pH. As the initial concentration increases, it is expected that adsorption percentages decrease as a consequence of the occupation of adsorption sites. At pH 2.0 and 6.0 the adsorption percentages are undistinguishable, around 80-90%, up to the

TABLE 1
TG/DTG data for FDU-1 AS, FDU-1 EX, FDU-1/HA AS and FDU-1/HA EX samples

	H_2O		Thermal decomposition of template/humic acid and dehydroxylation			
Samples	Δm_1 (%) [TR1 (°C)]	Tp_1 (°C)	Δm_2 (%) [TR2 (°C)]	Tp_2 (°C)	Δm_3 (%) [TR3 (°C)]	Tp_3 (°C)
FDU-1 AS	6.0 [25-124]	67	25 [124-211]	178	18 [211-1000]	246
FDU-1 EX	7.0 [22-230]	69	4.0 [133-300]	264	–	–
FDU-1 HA AS	4.0 [23-123]	63	34 [123-329]	249	13 [329-1000]	506
FDU-1 HA EX	16 [22-230]	89	5.0 [230-455]	326	5.0 [455-1000]	530

*Δm = mass loss of TG curves; Tp, peak temperature of DTG curve; TR, temperature range of TG event.

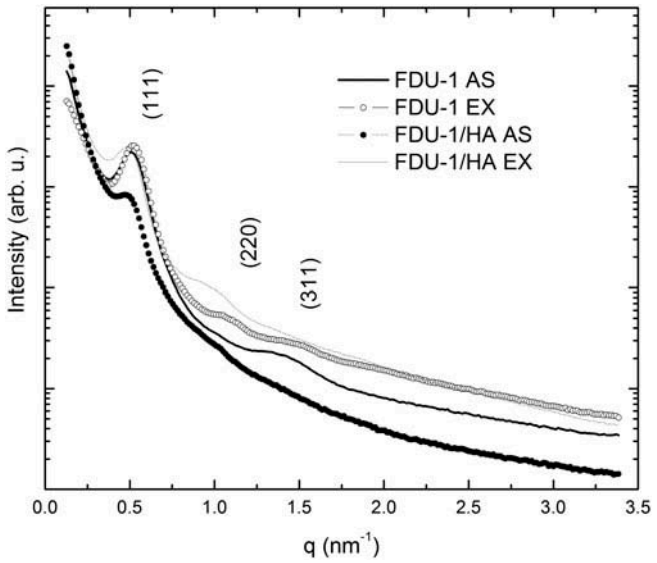

FIG. 2. Small angle X-ray scattering (SAXS) patterns for FDU-1 AS, FDU-1 EX, FDU-1/HA AS, and FDU-1/ HA EX samples.

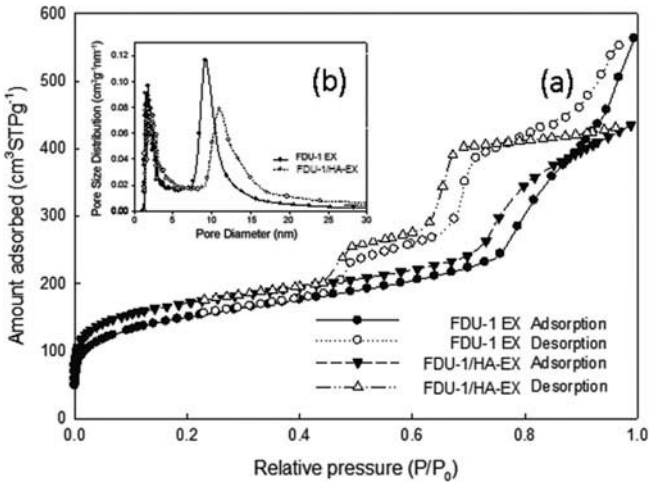

FIG. 3. Nitrogen adsorption isotherms at 77 K (a) and the corresponding pore size distributions (b) for FDU-1 EX and FDU-1/ HA EX samples.

initial Hg(II) concentration of 50 μmol L^{-1}. As the initial concentration increases, adsorption remains at around of 77% at pH 6.0, but decreases down to about 48% at pH 2.0, that is, there is a clear proton competition for the silanol groups as the pH is decreased from 6.0 to 2.0. Adsorption of Hg(II) on FDU-1 EX at pH 4.0 increases with the initial Hg(II) concentration from about 57 to 84%. The behavior at pH 4.0 is not clear, and may be related to interaction of Hg(II) with the acetate buffer affecting the adsorption on FDU-1 EX. Species $HgAc_4^{2-}$ prevails at pH < 4.0 (35), so that the acetate complex may inhibit adsorption at low Hg(II) concentrations, acting as a competitive ligand against adsorption by the silanol groups of FDU-1 EX. Competitive complexation of Hg(II) by chloride, humic, and fulvic acids inhibiting adsorption has been reported in the adsorption on polyaniline (9) and muscovite (21), and has to be considered in the further application of the FDU-1/HA EX to real water samples.

TABLE 2
Structural and textural properties of FDU-1 EX and FDU-1/HA EX

Sample	S_{BET} (m^2g^{-1})	V_{pt} (cm^3g^{-1})	V_M (cm^3g^{-1})	V_m (cm^3g^{-1})	w_{KJS} (nm)	a (nm)	b (nm)
FDU-1 EX	570	0.67	0.56	0.11	9.2	24.7	5.1
FDU-1/HA EX	513	0.87	0.80	0.07	10.3	25.1	3.7

S_{BET}, BET specific surface area; Vpt, total pore volume; V_M. total mesopore volume; Vm, total micropore volume; w_{KJS}, primary mesopore diameter; a, unit-cell parameters; b, average wall thickness.

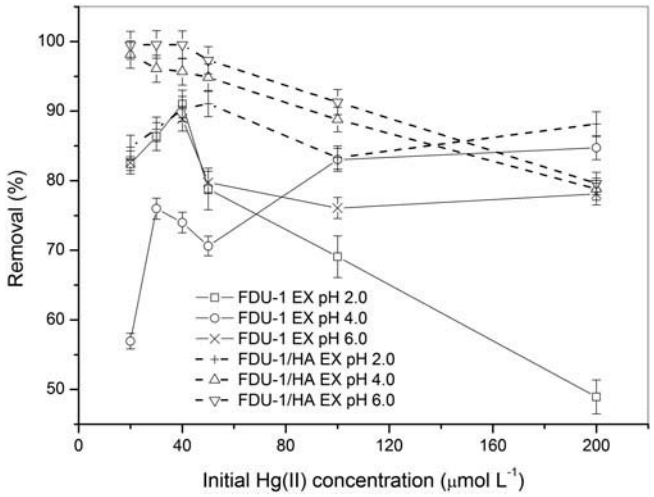

FIG. 4. Removal percentages of Hg(II) by adsorption FDU-1 EX and FDU-1/HA EX at pH 2.0, 4.0 and 6.0. Results are the mean of two experiments.

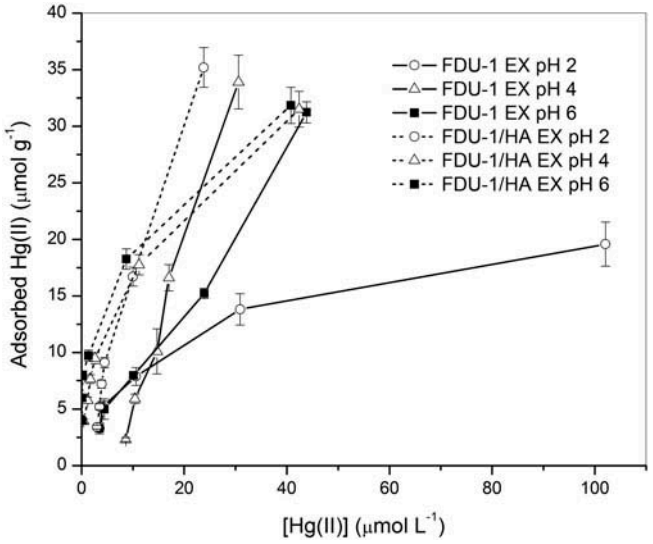

FIG. 5. Adsorption isotherms (25.0 ± 0.10°C) of Hg(II) on FDU-1 EX and FDU-1/HA EX materials at pH 2.0, 4.0, and 6.0. Results are the mean of two experiments.

Adsorption on FDU-1/HA EX is systematically higher than that on FDU-1 EX, independently of pH and initial concentration, especially at pH 4.0 and 6.0, a fact that may be explained by interaction of Hg(II) with the carboxylic and phenolic groups of the humic acid bound to the mesoporous silica. Adsorption on FDU-1/HA decreases from 98–99% to around 78–79% as the initial Hg(II) concentrations increase from 20 to 200 μmol L^{-1} (pH 4.0 and 6.0). At pH 2.0 the adsorption percentage on FDU-1/HA remains between 83 and 91%, independently of the initial of Hg(II) concentration. This behavior is consistent with the findings of Lee et al. (21), who described significant increase of Hg(II) binding by muscovite modified by pre-adsorption of fulvic acid. Pre-adsorbed humic acid onto FDU-1 has also been described as increasing adsorption of Cu(II), Cd(II), and Pb(II) in comparison with the non-modified material (20).

Figure 5 shows the adsorption isotherms for both FDU-1 EX and FDU-1/HA EX at the three studied pH. All isotherms were satisfactorily fitted to the linearized Freundlich equation (Table 3). Isotherms for the FDU-1 EX material at pH 4.0 and 6.0 were almost linear, indicating strong homogeneity of the adsorption sites ($1/n \rightarrow 1$), which is consistent with the predominance of silanol groups in the sorbent. On the other hand, at pH 2.0 a typical L-type adsorption curve was obtained ($1/n = 0.42 \pm 0.03$), indicating strong heterogeneity of the adsorption sites. Interpretation of the behavior is not clear, but it may be related, as already mentioned, to competition of Hg(II) with protons for the silanol groups, as well as heterogeneity of site accessibility (surface and inside the porous structure). Speciation of Hg(II) in solution also plays an important role because only at pH 2.0 the free aqueous Hg(II) prevails. At pH 4.0, $HgAc_4^{2-}$ is the dominant species, and, at pH 6.0 mixed contributions of $Hg(OH)_2$ and Hg(II)-MES complex may have influence on the adsorption.

Interpretation of adsorption data of Hg(II) on FDU-1/HA EX is straightforward: as the pH increases from 2.0 to 6.0, the K_f parameter increases from (1.2 ± 0.4) to (10.5 ± 1.0) $\mu mol^{1-1/n}L^{1/n}g^{-1}$ as a consequence of the lessened proton competition by the binding sites. The 1/n parameter decreases from (1.0 ± 0.1) to (0.27 ± 0.03) (Table 3), indicating an increase in the heterogeneity of binding sites (36, 37), a fact that is consistent with the silanol, carboxylic, and phenolic groups in the sorbent, as well as their increasing availability to interact with Hg(II) as the pH increases. In comparison with FDU-1 EX, enhancement of adsorption on FDU-1/HA EX is especially noticed at low Hg(II) concentrations (Fig. 5). This fact is explained by the larger affinity of carboxylic and phenolic groups by Hg(II) in relation to the silanol dominating groups in FDU-1 EX. Comparing the Freundlich parameters found in a previous work with Cu(II), Cd(II), and Pb(II) (20), one can infer that the selectivity of FDU-1/HA-EX towards Hg(II) is similar to that found to Cu(II), higher than for Cd(II), but lower than for Pb(II). As silanol, carboxylic, and phenolic groups form stable complexes with a variety of metal cations, a more rigorous selectivity study would be necessary before application of the materials for treatment of wastewaters, considering also the presence of major components in waters such as Mg(II) and Ca(II).

No attempt was made to investigate the total adsorption capacities for the two adsorbents under the three different pH, but, with exception of adsorption capacity of FDU-1 EX at pH 2, which is markedly smaller than the other conditions, the range of total Hg(II) concentrations between 20 and 200 μmol L^{-1} is far from saturating the adsorption sites. As the adsorption isotherms were obtained under low degree of site occupation it is difficult to compare adsorption capacities of the proposed

TABLE 3
Freundlich parameters for adsorption of Hg(II) on FDU-1 EX and FDU-1/HA EX

Material	Freundlich parameter	pH 2.0	pH 4.0	pH 6.0
FDU-1 EX	K_f	2.9 ± 0.3	0.23 ± 0.08	1.1 ± 0.2
	1/n	0.42 ± 0.03	1.5 ± 0.2	0.86 ± 0.05
	r	0.993	0.988	0.996
FDU-1/HA EX	K_f	1.2 ± 0.4	5.9 ± 0.2	10.5 ± 1.0
	1/n	1.0 ± 0.1	0.45 ± 0.02	0.27 ± 0.03
	r	0.985	0.998	0.988

materials with those of other adsorbents described in the literature. On the other hand, adsorption parameters obtained at low site occupation are more representative of total mercury concentrations found in waste and natural waters (36). Besides, low concentrations minimize the contribution of $Hg(OH)_2$ precipitation which is likely to occur if one attempts to find saturation of adsorption sites.

Comparing the K_f adsorption capacity parameter fitted by the Freundlich equation (Table 3), or the adsorbed amount for a given initial Hg(II) concentration, it is possible to state that the values found for the FDU-1/HA-EX are smaller than those described for thiol-functionalized mesoporous silicas (6, 17, 38). These capacity parameters, however, are of similar magnitude as those described for mesoporous silicas modified with 3–amino propyltriethoxysilane, 3-(2-aminoethyamino)propyldimethoxymethylsilane (39), and SBA-15 mesoporous silica modified with trithiane (40). The capacity of FDU-1/HA-EX is larger than those reported for SBA-15 silica modified with 1-(3-carboxyphenyl)-2-thiourea (41) and MCM-41 modified with $ZnCl_2$ (42). One of the main advantages of the proposed FDU-1/HA-EX silica is the one-step synthesis using an environmentally friendly and low cost humic modifier, contrary to post-synthesis with toxic silylation reagents containing thiol groups such as 3-mercaptotrimethoxysilane.

Desorption was sequentially studied in the adsorption medium (Fig 6a) and in 0.10 mol L^{-1} acetic acid (Fig 6b). Desorption isotherms were not described by the Freundlich equation, but allowed to evaluate the reversibility of the adsorption process. Figure 6a shows that adsorption of Hg(II) on FDU-1 EX at pH 2.0 was partially reversible, especially for the lower loads of Hg(II), indicating that at low initial Hg(II) concentrations, sorption occurs at the external surface, but as these sites are occupied, Hg(II) ions penetrate in the porous structure, being more strongly retained and less prone to desorption. A similar profile was observed for the FDU-1/HA EX material at pH 2.0, but with significantly lower percentages of desorption, which is explained by stronger interaction of Hg(II) with carboxylic and phenolic groups and formation of surface complexes (28). Desorption from FDU-1/HA EX at pHs 4.0 and 6.0 was negligible, suggesting that adsorption is governed by chemisorption, probably by surface complexation of Hg(II) with silanol, carboxylic, and phenolic groups.

Desorption in 0.10 mol L^{-1} acetic acid (Fig 6b) is significant from the FDU-1 EX material submitted to adsorption/desorption at pH 6.0. This behavior is consistent with protonation of silanol sites and $Hg(OH)^+$ or $Hg(OH)_2$ species adsorbed either on the surface or in the mesopores. Desorption percentages from the FDU-1 decreased for the materials studied at pH 4.0 and 2.0 (Fig 6b), which is consistent with the behavior of silanol groups that were predominantly protonated in the adsorption study. Besides, the presence of hydrolytic species of Hg(II) are negligible at pH 2.0 or 4.0. Desorption of Hg(II) in acetic acid did not exceed 1% of the amount of Hg(II) that remained adsorbed in FDU-1/HA after the adsorption/desorption experiments made at pH 2.0, 4.0, or 6.0. This fact gives support for the hypothesis that the interaction of Hg(II) with the FDU-1/HA EX material is strong, governed by chemisorption (complexation with silanol, carboxylic, and phenolic groups), and is not prone to desorption upon pH lowering and proton competition. These characteristics make the FDU-1/HA EX material a strong adsorbent for Hg(II), having potential application in the removal of this ion from contaminated waters.

CONCLUSIONS

The one-pot synthesis described in this paper, which produced an adsorbent with humic acid on cage-like ordered mesoporous silica, FDU-1 type, proved to be an efficient absorbent of Hg(II). The increase on the affinity of this new adsorbent for Hg(II) ions is a consequence of incorporation of carboxylic and phenolic groups. Adsorption was predominantly irreversible, as evidenced by the leaching experiments. The pre-adsorbed Hg(II) desorption percentages were smaller than 10%, suggesting that chemisorption is the predominant adsorption process governing the removal of Hg(II) from solution. These materials have potential application in water treatment and in analytical chemistry as concentrators of heavy metals. Future

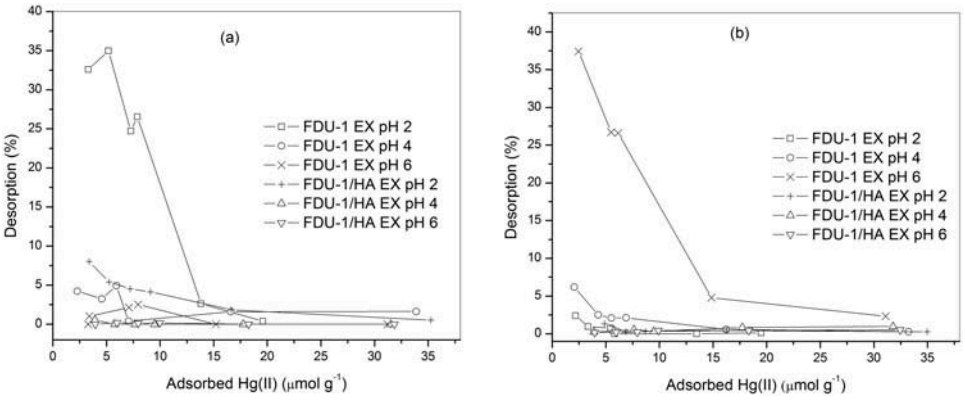

FIG. 6. Desorption percentages from FDU-1 EX and FDU-1/HA EX materials obtained from 24 h desorption experiments (25.0 ± 0.10°C) made in the adsorption medium (a), followed by 2 h desorption in 0.10 mol L^{-1} acetic acid (b). Results are themean of two experiments.

work with FDU-1 is the incorporation of amine and thiol groups aiming further enhancement in its adsorption capacity toward heavy metals, as well as studying the influence of Hg(II) speciation in the presence of common ligands such as chloride and dissolved organic matter on the adsorption/desorption processes.

FUNDING

The authors are grateful to the São Paulo Research Foundation (FAPESP, Project number 2007/07646-2) and Conselho Nacional de Desenvolvimento Científico e Tecnológico (CNPq, Project numbers 475554/2009-4 and 304178/2009-8) for the financial support and fellowships.

REFERENCES

1. Rafaj, P.; Bertok, I.; Cofala, J.; Schöpp, W. (2013) Scenarios of global mercury emissions from anthropogenic sources. *Atmos. Environ*., 79: 472.
2. Costa, M. F.; Landing, W. M.; Kehrig, H. A.; Barletta, M.; Holmes, C. D.; Barrocas, P.R.G.; Evers, D. C.; Buck, D. G.; Vasconcellos, A. C.; Hacon, S. S.; Moreira, J. C.; Malm O. (2012) Mercury in tropical and subtropical coastal environments. *Environ. Res*., 119: 88.
3. Reddy, K. S. K.; Al Shoaibi, A.; Srinivasakannan, C. (2014) Elemental mercury adsorption on sulfur-impregnated porous carbon: A review. *Environ. Technol*., 35: 18.
4. Johari, K.; Saman, N;. Mat, H. (2014) Adsorption enhancement of elemental mercury onto sulphur-functionalized silica gel adsorbents. *Environ. Technol*., 35: 629.
5. De, M.; Azargohar, R.; Dalai, A. K.; Shewchuk, S. R. (2013) Mercury removal by bio-char based modified activated carbons. *Fuel*, 103: 570.
6. Walcarius, A.; Etienne, M.; Delacote, C. (2004) Uptake of inorganic Hg(II) by organically modified silicates: influence of pH and chloride concentration on the binding pathways and electrochemical monitoring of the processes. *Anal. Chim. Acta*, 508: 87.
7. Liu, M.; Hou, L.; Xi, B.; Zhao, Y.; Xia, X. (2013) Synthesis, characterization, and mercury adsorption properties of hybrid mesoporous aluminosilicate sieve prepared with fly ash. *Appl. Surf. Sci*., 273: 706.
8. Velikova, N.; Vueva, Y.; Ivanova, Y.; Salvado, I.; Fernandes, M.; Vassileva, P.; Georgieva, R.; Detcheva, A. (2013) Synthesis and characterization of sol–gel mesoporous organosilicas functionalized with amine groups. *J. Non-Cryst. Solids*, 378: 89.
9. Wang, J.; Deng, B.; Chen, H.; Wang, X.; Zheng, J. (2009) Removal of aqueous Hg(II) by polyaniline: sorption characteristics and mechanisms. *Environ. Sci. Technol*., 43: 5223.
10. Samandari, S. S.; Gazi, M. (2013) Removal of mercury (II) from aqueous solution using chitosan-graft-polyacrylamide semi-IPN hydrogels. *Sep. Sci. Technol*., 48 1382.
11. Sarı, A.; Tüzen M.; Cıtak, D. (2012) Equilibrium, thermodynamic and kinetic studies on biosorption of mercury from aqueous solution by macrofungus (*Lycoperdon perlatum*) biomass. *Sep. Sci. Technol*., 47: 1167.
12. Wang, Y.; Qi, Y.; Li, Y.; Wu, J.; Ma, X.; Yu, C.; Ji, L. (2013) Preparation and characterization of a novel nano-absorbent based on multi-cyanoguanidine modified magnetic chitosan and its highly effective recovery for Hg(II) in aqueous phase. *J. Hazard. Mat*., 260: 9.
13. Wanga, X.; Sun, R.; Wang, C. (2014) pH dependence and thermodynamics of Hg(II) adsorption onto chitosan-poly(vinyl alcohol) hydrogel adsorbent. *Colloid Surface A*, 441: 51.
14. Jiskra, M.; Wiederhold, J.G.; Bourdon. B.; Kretzschmar, R. (2012) Solution speciation controls mercury isotope fractionation of Hg(II) sorption to goethite. *Environ. Sci. Technol*., 46: 6654.
15. Ding, F.; Zhao, Y.; Mi, L.; Li, H.; Li Y.; Zhang, J. (2012) Removal of gas-phase elemental mercury in flue gas by inorganic chemically promoted natural mineral sorbents. *Ind. Eng. Chem. Res*., 51: 3039.
16. Guerra D. L.; Santos, M. R. M. C.; Airoldi, C. (2009) Mercury adsorption on natural and organofunctionalized smectites: Thermodynamics of cation removal. *J. Braz. Chem. Soc*., 20: 594.
17. Delacôte, C.; Gaslain, F.O.M.; Lebeau, B.; Walcarius, A. (2009) Factors affecting the reactivity of thiol-functionalized mesoporous silica adsorbents toward mercury(II). *Talanta*, 79: 877.
18. Busche, B.; Wiacek, R.; Davidson, J.; Koonsiripaiboon, V.; Yantasee, W.; Addleman, R. S.; Fryxell, G. E. (2009) Synthesis of nanoporous iminodiacetic acid sorbents for binding transition metals. *Inorg. Chem. Commun*., 12: 312.
19. Cides da Silva, L. C.; Abate, G.; Andrea, N. A.; Fantini, M. C. A.; Masini, J. C.; Mercuri, L. P.; Olkhovyk, O.; Matos, J. R. (2005) Microwave synthesis of FDU-1 silica with incorporated humic acid and its applications for adsorptions of Cd^{2+} from aqueous solutions. *Stud. Surf. Sci. Catal*., 156: 941.
20. Cides da Silva, L. C.; dos Santos, L. B. O.; Abate, G.; Cosentino, I. C.; Fantini, M. C. A.; Masini, J. C.; Matos, J. R. (2008) Adsorption of Pb^{2+}, Cu^{2+} and Cd^{2+} in FDU-1 silica and FDU-1 silica modified with humic acid. *Micropor. Mesopor. Mater*., 110: 250.
21. Lee, S. S.; Nagy, K. L.; Park, C.; Fenter, P. (2009) Enhanced uptake and modified distribution of mercury(II) by fulvic acid on the muscovite (001) surface. *Environ. Sci. Technol*., 43: 5295.
22. Yu, C.; Yu, Y.; Zhao, D. (2000) Highly ordered large caged cubic mesoporous silica structures templated by triblock PEO–PBO–PEO copolymer. *Chem. Commun*., 7: 575.

23. Yu, C.; Tian, B.; Fan, J.; Stucky, G. D.; Zhao, D. (2002) Nonionic block copolymer synthesis of large-pore cubic mesoporous single crystals by use of inorganic salts. *J. Am. Chem. Soc*., 124: 4556.
24. Kruk, M.; Celer, E. B.; Jaroniec, M. (2004) Exceptionally high stability of copolymer-templated ordered silica with large cage-like mesopores. *Chem. Mater*., 16: 698.
25. Matos, J. R.; Kruk, M.; Mercuri, L. P.; Jaroniec, M.; Zhao, L.; Kamiyama, T.; Terazaki, O.; Pinnavaia, T. J.; Liu, Y. (2003) Ordered mesoporous silica with large cage-like pores: structural identification and pore connectivity design by controlling the synthesis temperature and time. *J. Am. Chem. Soc*. 125: 821.
26. Fantini, M. C. A.; Matos, J. R.; Cides da Silva, L. C.; Mercuri, L. P.; Chiereci, G. O.; Celer, E.; Jaroniec, M. (2004) Ordered mesoporous silica: Microwave synthesis. *Mat. Sci. Eng. B*, 112:106.
27. Cides da Silva, L. C.; dos Reis, T. V. S.; Cosentino, I. C.; Fantini, M. C. A.; Matos, J. R.; Bruns, R. E. (2010) Factorial design to optimize microwave-assisted synthesis of FDU-1 silica with a new triblock copolymer. *Micropor. Mesopor. Mater*., 133: 1.
28. Vasiliev, A.N.; Golovko, L.V.; Trachevsky, V.V.; Hall, G.S.; Khinast, J.G. (2009) Adsorption of heavy metal cations by organic ligands grafted on porous materials. *Micropor. Mesopor. Mater*., 118: 251.
29. Brunauer, S.; Emmet, P. H.; Teller, E. (1938) Adsorption of gases in multimolecular layers. *J. Am. Chem. Soc*., 60: 309.
30. Barret, E. P.; Joyner, L. G.; Halenda, P. H. (1951) The determination of pore volume and area distributions in porous substances. I. Computations from nitrogen isotherms. *J. Am. Chem. Soc*., 73: 373.
31. Kruk, M.; Jaroniec, M.; Sayari, A. (1997) Application of large pore MCM-41 molecular sieves to improve pore size analysis using nitrogen adsorption measurements. *Langmuir*, 13: 6267.
32. Chekmeneva, E.; Díaz-Cruz, J. M.; Ariño, C.; Esteban, M. (2009) Use of rotating Au-thin film electrode for the differential pulse voltammetric study of Hg^{2+} complexation. *J. Electroanal. Chem*., 629: 169.
33. Giacomino, A.; Abollino, O.; Malandrino, M.; Mentasti, E. (2008) Parameters affecting the determination of mercury by anodic stripping voltammetry using a gold electrode. *Talanta*, 75: 266.
34. Bonfil, Y.; Brand, M.; Kirowa-Eisner, E. (2000) Trace determination of mercury by anodic stripping voltammetry at the rotating gold electrode. *Anal. Chim. Acta*, 424: 65.
35. Nam, K. H.; Gomez-Salazar, S.; Tavlarides, L. L. (2003) Mercury(II) adsorption from wastewaters using a thiol functional adsorbent. *Ind. Eng. Chem. Res*., 42: 1955.
36. Buffle, J. (1990) *Complexation Reactions in Aquatic Systems: An Analytical Approach;* Ellis Horwood Limited: Chichester, UK.
37. Abate, G.; Masini, J. C. (2002) Complexation of Cd(II) and Pb(II) with humic acids studied by anodic stripping voltammetry using differential equilibrium functions and discrete site models. *Org. Geochem*., 33: 1171.
38. Ravi, S.; Selvaraj, M.; Park, H.; Chun, H.-H.; Ha, C.-S. (2014) Novel hierarchirally dispersed mesoporous silica spheres: effective adsorbents for mercury from waters and a thermodynamic study. *New J. Chem*., 38: 3899.
39. Zhu, Z.; Yang, X.; He, L-N.; Li, W. (2012) Adsorption of Hg^{2+} from aqueous solution on functionalized MCM-41. *RSC Adv*., 2: 1088.
40. Bidhendi, M. E.; Bidhendi, G. R. N.; Mehrdadi, N.; Rashedi, H. (2014) Modified mesoporous silica (SBA-15) with trithiane as a new effective adsorbent for mercury ions removal from aqueous environment. *J. Environ. Health Sci. Eng*., 12:100.
41. Zhang, L.; Sheena, G.; Hu, X.; Crawford, R.; Yu, A. (2012) Removal of aqueous toxic Hg(II) functionalized mesoporous silica materials. *J. Chem. Technol. Biotechnol*., 87: 1473.
42. Raji, F.; Pakizeh, M. (2014) Kinetic and thermodynamic studies of Hg(II) adsorption onto MCM-41 modified with $ZnCl_2$. *Appl. Surf. Sci*., 301: 568.